Wiesław ŁYSKAWIŃSKI

FINITE ELEMENT ANALYSIS OF EDDY CURRENT LOSSES IN PULSE TRANSFORMER

ABSTRACT *In the paper an algorithm for power loss determination in pulse transformers using a field-circuit model is described. The software based on the algorithm is used to calculate eddy current losses and determine efficiency of a pulse transformer. Eddy current power losses and efficiency of a pulse transformer for different load resistances, input signal shapes and lengths of the central leg of the core are analysed. Selected results of simulations are shown.*

Keywords: *pulse transformer, eddy current losses, FEM analysis*

1. INTRODUCTION

Pulse transformers are core components of most electronic devices and they impact immensely on both their efficiency and reliability. The appropriate design of pulse transformers needs, therefore, to be aimed at obtaining minimum

Wiesław ŁYSKAWIŃSKI, Ph.D.

Poznan University of Technology,
Institute of Industrial Electrical Engineering,
Electrical MachinesDept,
Piotrowo 3A, 60-965 Poznan, POLAND,
tel. +(48-61)6652116, fax: +(48-61) 6652389,
e-mail: Wieslaw.Lyskawinski@put.poznan.pl

PROCEEDINGS OF ELECTROTECHNICAL INSTITUTE, Issue 229, 2006

power losses, high efficiency and low temperature rise. Power losses are generated in the form of waste heat that causes the temperature in the system to rise. Much research is being conducted to limit these drawbacks. The losses are mainly due to skin effect, conductor proximity (eddy current losses) and capacitive currents (dielectric losses in the winding). The circuital models proposed in the literature of the subject offer merely an approximate rendition of these phenomena [3, 6, 7, 9], and precise modelling is only possible if field methods are applied [4]. The present paper propounds a field-circuit model of determining eddy current power losses of pulse transformers.

2. EDDY CURRENT POWER LOSS CALCULATION

The eddy current power losses ΔP in a pulse transformer can be determined from the temporal and spatial distribution of current density vector

$$\Delta P = \int_V \frac{1}{\gamma}\left[\frac{1}{T}\int_0^T j^2(\rho, z, t)\,dt\right]dV \tag{1}$$

where γ is the conductivity, T is the current density j period, V is the considered region volume (core, windings).

Loss calculation based on the dependence (1) is not an easy task because generally in voltage-excited systems with non-linear elements the course and distribution of current density in the windings and eddy currents in the core are not known in advance [2, 5]. A field-circuit model of pulse transformers is used [4] for the calculation of these currents. The model includes the equations of the electromagnetic field and the equations describing current in electric circuits. The equations of the electric circuit of the pulse transformer and the equations of supply circuits may be written as

$$\boldsymbol{u} = \boldsymbol{R}\boldsymbol{i} + \frac{d}{dt}\boldsymbol{\Psi} + \boldsymbol{L}_z\frac{d}{dt}\boldsymbol{i} + \boldsymbol{C}_z\int_0^t \boldsymbol{i}\,dt \tag{2}$$

where $\boldsymbol{u}$ is the vector of supply voltages, $\boldsymbol{i}$ is the vector of loop currents, $\boldsymbol{R}$ is the matrix of loop resistances, $\boldsymbol{L}$ is the matrix of inductances, $\boldsymbol{\Psi}$ is the flux linkage vector calculated on the basis of field distribution, $\boldsymbol{L}_z$, $\boldsymbol{C}_z$ are the inductance and elastance matrixes of the supply system.

In the paper, a pulse transformer with axial symmetry is considered (Fig. 1). A cylindrical coordinate system ρ, z, ϑ was applied. In this case, equation describing the transient electromagnetic field in the transformer can be expressed as

$$\frac{\partial}{\partial\rho}\left(\frac{1}{\mu l}\frac{\partial\varphi}{\partial\rho}\right)+\frac{\partial}{\partial z}\left(\frac{1}{\mu l}\frac{\partial\varphi}{\partial z}\right)=J-\frac{\gamma}{l}\frac{d\varphi}{dt} \tag{3}$$

Here $l=2\pi\rho$, $\varphi=2\pi\rho A_\vartheta$, where A_ϑ is the auxiliary magnetic potential, J is the current density in the ϑ-direction.

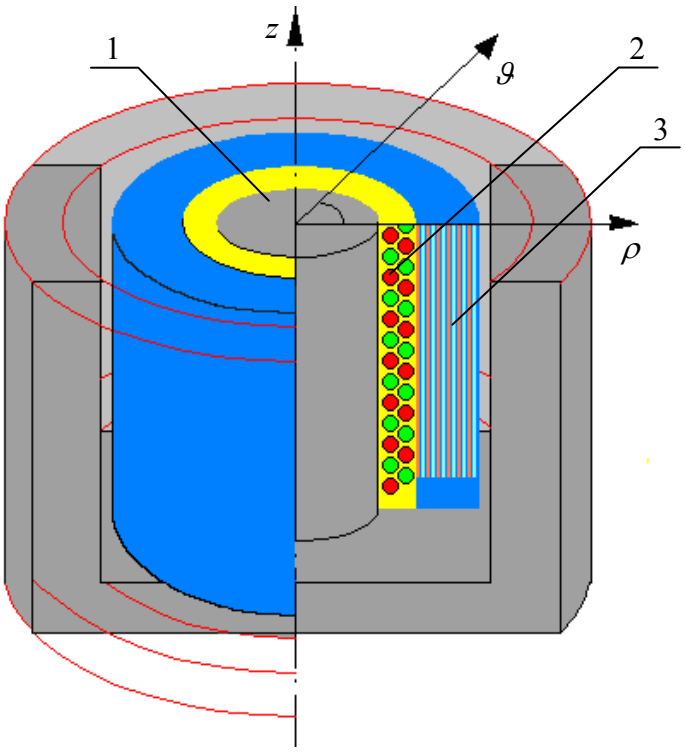

Fig. 1. Pulse transformer 1- ferrite core, 2- primary winding, 3- secondary winding

3. FINITE ELEMENT FORMULATION

Non-linearity of equations (2), (3) together with the complicated structure of transformer render it impossible to analytically solve the equations of the

presented model. Only approximate methods can be applied, based on the discretization of space and time [2, 5]. In the paper numerical implementation of the mathematical model based on the finite element method and a step-by-step procedure is proposed. The backward difference scheme has been applied. The finite element and time discretization lead to the following system of non-linear algebraic matrix equations [2, 4]

$$\begin{bmatrix} \boldsymbol{M}_n & -\boldsymbol{N} \\ -\boldsymbol{N}^{\mathrm{T}} & -\Delta t\boldsymbol{Z} \end{bmatrix} \begin{bmatrix} \boldsymbol{\varphi}_n \\ \boldsymbol{i}_n \end{bmatrix} = \begin{bmatrix} (\Delta t)^{-1}\boldsymbol{G}(1-\boldsymbol{K})\boldsymbol{\varphi}_{n-1} \\ -\Delta t\boldsymbol{u}_n + \tilde{\boldsymbol{\psi}}_{n-1} \end{bmatrix} \tag{4}$$

where:

$$\boldsymbol{M}_n = \boldsymbol{S}_n + (\Delta t)^{-1}\boldsymbol{G}(1-\boldsymbol{K}),$$
$$\boldsymbol{Z} = \boldsymbol{R} + \Delta t\boldsymbol{C}_z + (\Delta t)^{-1}\boldsymbol{L}_z,$$
$$\tilde{\boldsymbol{\psi}}_{n-1} = -\boldsymbol{N}^{\mathrm{T}}\boldsymbol{\varphi}_{n-1} - (\Delta t)^{-1}\boldsymbol{L}_z\boldsymbol{i}_{n-1} + \Delta t\boldsymbol{u}_{cn-1},$$

n denotes the number of time-step, Δt is the time-step length, $\boldsymbol{\varphi}$ is the vector of nodal potentials, $\boldsymbol{N}^{\mathrm{T}}$ is the matrix that transforms the potentials $\boldsymbol{\varphi}$ into the flux linkages with the windings, $\boldsymbol{G}$ is the matrix of conductances of elementary rings formed by mesh, $\boldsymbol{S}$ is the stiffness matrix, $\boldsymbol{K}$ is the matrix consisting of diagonally placed sub-matrixes whose elements equal the ratio of the cross-section area of the fibre assigned to a given node to the cross-section area of the wire in this node, $\boldsymbol{u}_{cn-1}$ is the vector of the voltage on the capacitances at the n-1 time step.

The set of non-linear algebraic equations is solved by the iterative Newton-Raphsona method [1, 10]. One receives the distribution of equivalent magnetic potential and density of eddy currents in the core and currents in the windings. In the algorithm the calculated current density distributions derived from (1) are used to determine eddy current power losses in the core and power losses in the windings.

4. RESULTS

The algorithm is used to develop a computer program for determining power losses and efficiency of pulse transformers. A 240 W transformer with the ETD 44 core made from N 67 ferrite is considered (Fig. 1). Non-linear properties of magnetic materials and eddy currents induced in the core and the windings are taken into account.

The transformer is loaded with the resistance R_o. For $R_o = R_n$ rated load current is achieved. Since the range of the values of the relative load resistance $r = R_o/R_n$ was large, data in the charts are presented on a logarithmic scale. The impact of the changes of the relative load resistance r and the shape of input signal on the relative power losses in the windings $p_w = \Delta P_w / \Delta P_{wn}$ (Fig. 2) and in the core $p_c = \Delta P_c / \Delta P_{cn}$ (Fig. 3) as well as on the efficiency η of the transformer (Fig. 6) is calculated. Both sinusoidal and rectangular voltage sources are considered. Therefore, the relative power losses p_{wi}, p_{ci} for impulse supply voltage and p_{ws}, p_{cs} for sinusoidal supply voltage are distinguished. For efficiency calculation hysteresis losses are taken into account. They are approximated from catalogue data [8]. This efficiency for loads lower than the rated and measured efficiency of the transformer in pulse-excited power system is compared (Fig. 4). Good convergence of this two efficiency curves are obtained. It is established that the operating conditions of the transformer are optimal at the relative load resistance r = 1. For this value the efficiency of the transformer is at its highest (Fig. 6), and the losses in the windings and the core are low. At increasing load (r < 1) the losses accumulate quickly for impulse supply voltage and for load resistances lower than secondary winding resistances they stabilise at a certain level. For sinusoidal voltage the losses in the windings for r = 1 are similar to those for impulse voltage, and for very low load resistances they are three times lower. It is due to the fact that lower electromotive power is induced in the secondary winding at high load currents.

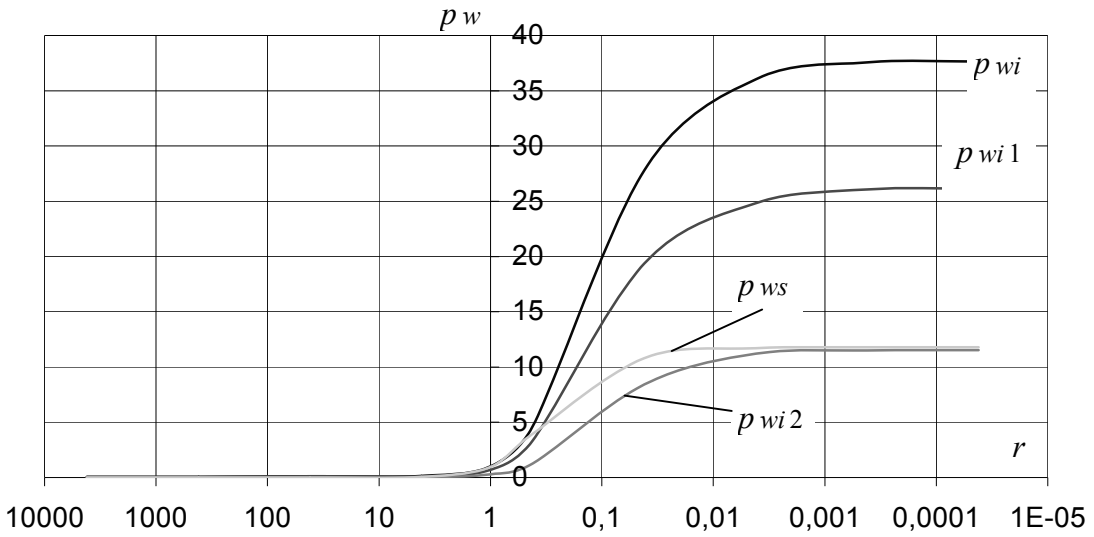

Fig. 2. Relative windings losses for rectangular $p_{wi}(r)$ and sinusoidal $p_{ws}(r)$ supply voltage

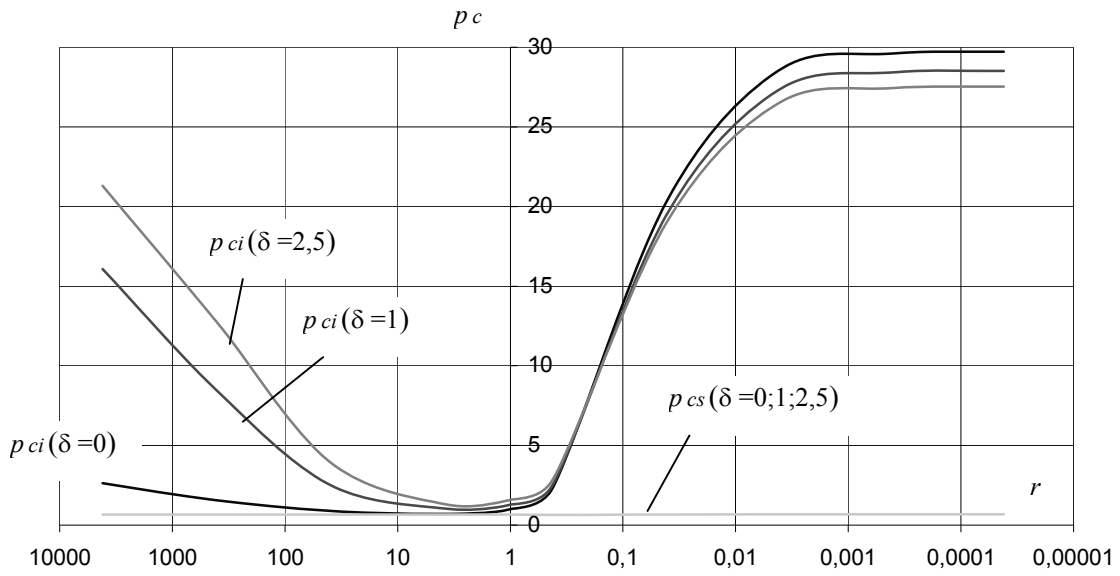

Fig. 3. Relative core losses for rectangular $p_{ci}(r)$ and sinusoidal $p_{cs}(r)$ supply voltage depends on the gap length δ = const [mm]

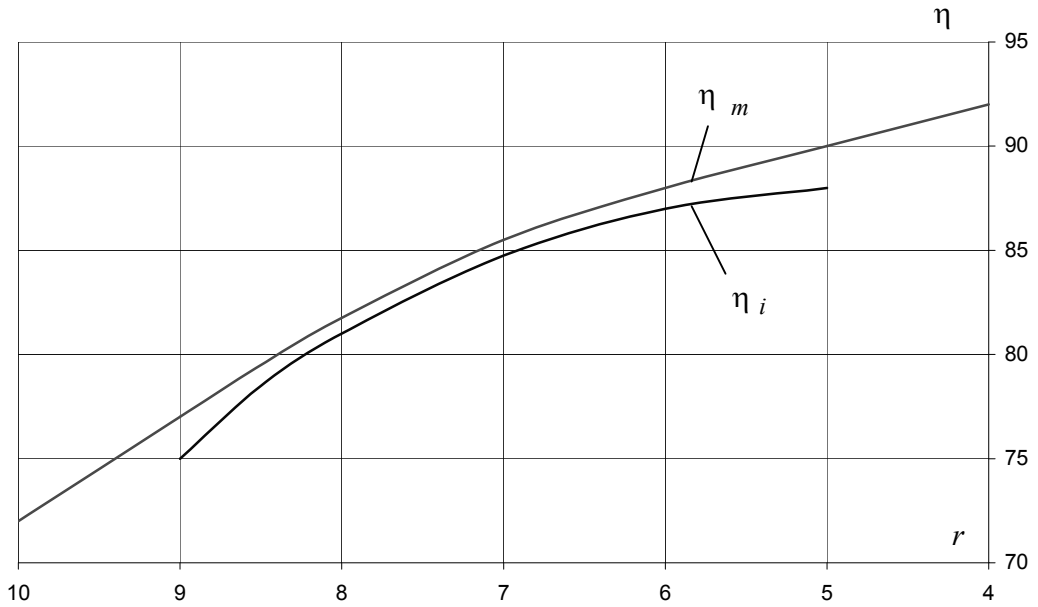

Fig. 4. Efficiency calculation $\eta_i(r)$ and measurement $\eta_m(r)$ for impulse supply voltage

The relative eddy current losses in the core p_{ci} are lowest for r = 1 ÷ 10, i.e. in the predicted operating range of the transformer. A similar value of the losses p_{cs} is achieved. In this case the losses p_{cs} are almost independent of load changes. For impulse supply voltage the losses p_{ci} increase for r > 10 and r < 1, and the curve $p_{ci}(r)$ depends on the gap length. The increase in the losses p_{ci}

compared with the losses p_{cs} for $r > 10$ is connected with greater dynamics of current changes in windings, and, consequently, with the changes of the magnetic field for impulse supply voltage. Additionally, for larger gaps the heterogeneity of the magnetic field in the core also increases. What follows is the increase of eddy current density and eddy current losses.

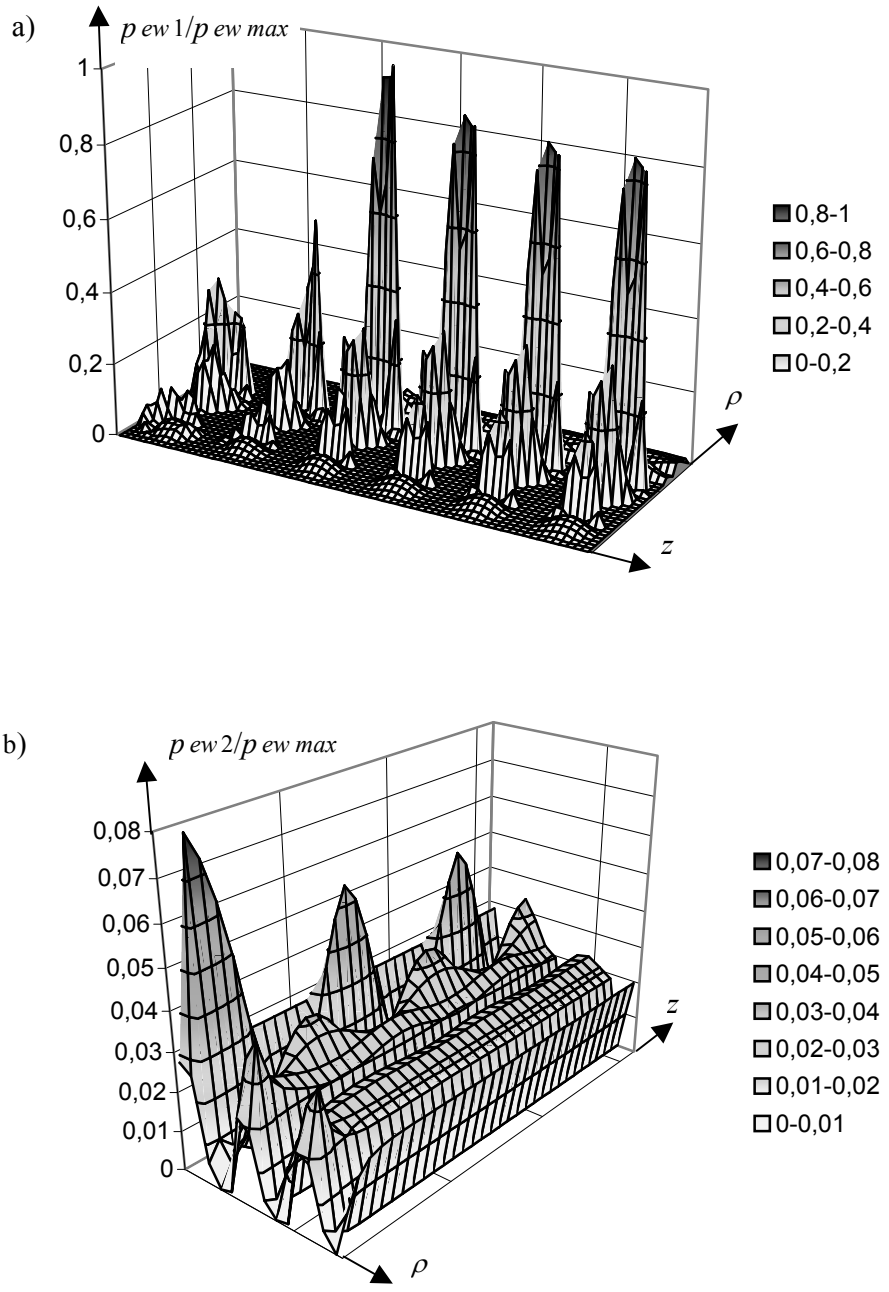

Fig. 5. Eddy current losses distributions in primary (a) and secondary (b) winding for region A from Fig. 7 after power-on in time $t = 0.03T$ (where T is the rectangular voltage period)

A sample eddy current losses distributions in chosen turns of primary and secondary winding after the application of pulse voltage are presented in Fig. 5. Maximum value of these losses occurs in parts of turns of primary winding adherent to secondary winding. This is due to the fact that in the boundary between primary and secondary winding magnetomotive force reach maximum. This region occurs a very dense magnetic field lines after the application of pulse voltage (Fig. 7).

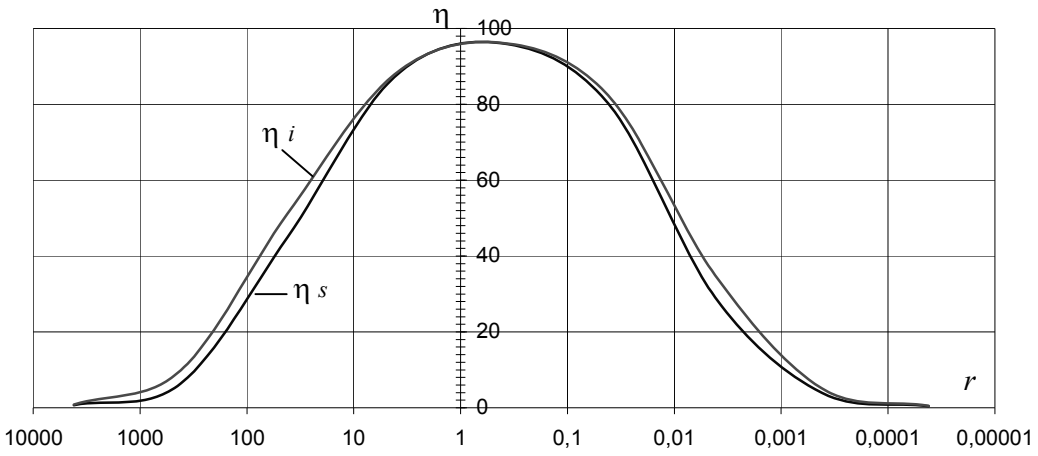

Fig. 6. Efficiency for rectangular $\eta_i(r)$ and sinusoidal $\eta_s(r)$ supply voltage

Maximum efficiency for the impulse supply η_i and the sinusoidal supply η_s does not differ much and amounts to c. 96 %. For loads higher and lower than the rated load the efficiency of the system decreases, though the decrease is more significant for sinusoidal supply. This is due to the fact that the rated load is not affected by the supply voltage type since similar efficiency is achieved in both cases. In practical solutions rectangular supply voltage is preferred because constant values of input voltage can be achieved in a wide range of load values through the adjustment of impulse width.

Time-variations of relative eddy current losses in the windings for one period T for non-load transformer during steady state are presented in Fig. 8. Increase of the gap results in the significant growth of the eddy current losses.

When the power is supplied, a significant impact of eddy currents on the distribution of the magnetic field can be observed. The field directly after power-on is concentrated around the windings that excite these currents.

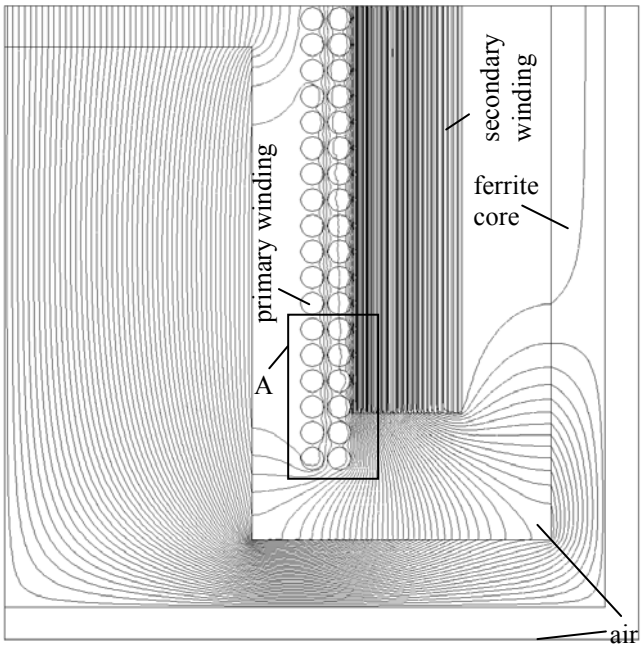

Fig. 7. Distribution of magnetic field lines in the considered region of pulse transformer after power-on (*t* = 0.03*T*) on the gap length δ = 2,5 [mm]

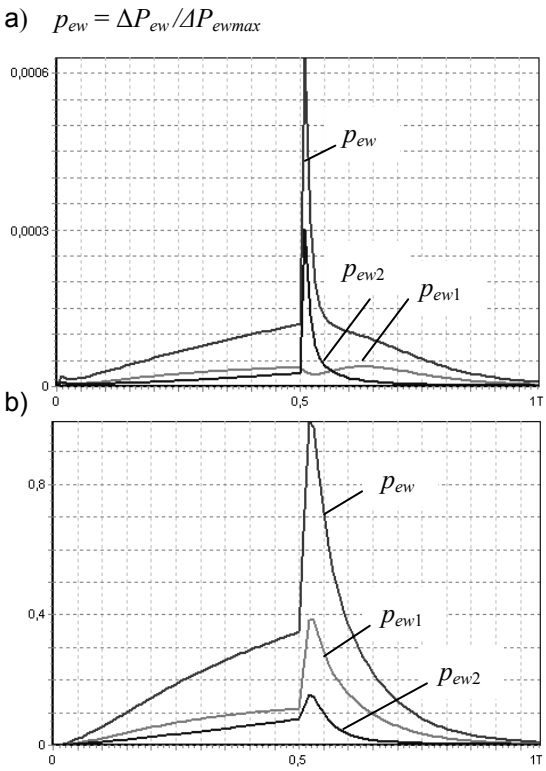

Fig. 8. Relative eddy current power losses waveforms in the windings during power-on (t=0) and power-off (t=0,5T) for the gap length δ = 0 (a), δ =2,5 [mm] (b)

5. CONCLUSION

In the paper a field-circuit model of electromagnetic phenomena in a high-frequency pulse transformer is presented. An algorithm for solving the equations of the model is suggested. The nonlinearity of the ferrite core and eddy currents excited in the core and the windings are taken into consideration. The algorithm is applied to develop a computer program that calculate eddy current losses in a pulse transformer. It is shown that the elaborated program can be used to analyse of eddy current losses in the core, power losses in the windings and efficiency of the transformer. The analyses of eddy current losses distributions in primary and secondary winding after the application of pulse voltage are presented. Good agreement between calculation and measurement efficiency curves is obtained. The software enables the analysis of losses in windings and cores of pulse transformers and can be used in the design and optimalisation of such transformers.

LITERATURE

1. Besbes M., Ren Z., Razek A.: *Finite element analysis of magnetomechanical coupled phenomena in magnetostrictive materials*, IEEE Transactions on Magnetics, Vol. 32, No. 3, pp. 1058-1061, May 1996.
2. Demenko A.: *Symulacja dynamicznych stanów pracy maszyn elektrycznych w ujęciu polowym*, Wydawnictwo Politechniki Poznańskiej, Poznań1997.
3. Laouamri K., Keradec J.-P., Member, IEEE, Ferrieux J.-P., Barbaroux J.: *Dielectric losses of capacitor and ferrite core in an LCT component*, IEEE Transactions on Magnetics, Vol. 39, No. 3, pp 1574-1577, May 2003.
4. Łyskawiński W.: *Field-circuit transient analysis of pulse-excited transformer*, Proc. EPNC2004, Poznań, pp. 49-50, June 2004.
5. Nowak L.: *Modele polowe przetworników elektromechanicznych w stanach nieustalonych*, Wydawnictwo Politechniki Poznańskiej, Poznań 1999.
6. Rumatowski K.: *Straty mocy w uzwojeniach transformatorów zasilaczy impu*lsowych, Wydawnictwo Politechniki Poznańskiej, Poznań 2002.
7. Schellmanns A., Berrouche K., Keradec J.-P.: *Multiwinding transformers: a successive refinement method to characterize a general equivalent circuit*, IEEE Transactions on Instrumentation and Measurement, Vol. 47, No. 5, pp. 1316-1321, October 1998.
8. Siemens Matsushita Components: *Ferrite core*, EPCOS, data book 1999.
9. Sullivan C. R.: *Computationally efficient winding loss calculation with multiple windings, arbitrary waveforms, and two-dimensional or three-dimensional field geometry*, IEEE Transactions on Power Electronics, Vol. 16, No. 1, pp. 142-150, January 2001.
10. Szeląg W.: *Demagnetization effects due to armature transient currents in the permanent magnet self starting synchronous motor*, Proc. EMF2000, Gent, pp. 93-94, May 2000.

Manuscript submitted 14.11.2006
Reviewed by Jerzy Zadrożny

ANALIZA STRAT WIROPRĄDOWYCH W TRANSFORMATORZE IMPULSOWYM METODĄ ELEMENTÓW SKOŃCZONYCH

W. ŁYSKAWIŃSKI

STRESZCZENIE *Wiroprądowe straty mocy ΔP w transformatorze impulsowym można wyznaczyć na podstawie czasowego przebiegu oraz przestrzennego rozkładu wektora gęstości prądu z zależności (1). Obliczanie tych strat jest jednak zagadnieniem trudnym, ponieważ w ogólnym przypadku przy wymuszeniu napięciowym w układach zawierających elementy nieliniowe nie jest znany a priori przebieg i rozkład gęstość prądu w uzwojeniach i prądów wirowych w rdzeniu. W celu wyznaczenia tych prądów posłużono się modelem polowo-obwodowym transformatora impulsowego. Model ten obejmuje równania pola elektromagnetycznego (3) i równania opisujące rozpływ prądów w obwodach elektrycznych (2). Ze względu na nieliniowość, szybką zmienność pola w czasie oraz złożoną strukturę równań tych nie można rozwiązać analitycznie. W tym celu wykorzystuje metodę elementów skończonych, polegającą na dyskretyzacji przestrzeni i czasu. W wyniku uzyskuje się układ nieliniowych równań algebraicznych (4).*

Do rozwiązania tego układu równań wykorzystuje się iteracyjną metodę Newtona-Raphsona. Na podstawie obliczonych rozkładów gęstości prądów z zależności (1) wyznacza się wiroprądowe straty mocy w rdzeniu i straty mocy w uzwojeniach.

Na podstawie przedstawionego algorytmu opracowano program do wyznaczania wiroprądowych strat mocy i sprawności w transformatorze impulsowym. Rozpatrzono transformator o mocy 240 W z rdzeniem ETD 44 wykonanym z ferrytu N 67 o strukturze przedstawionej na rys. 1. W rozważaniach uwzględniono nieliniowe właściwości materiałów magnetycznych oraz prądy wirowe indukujące się w rdzeniu i uzwojeniach.

Transformator obciążono rezystancją R_o. Dla $R_o = R_n$ uzyskano znamionowy prąd obciążenia. Ze względu na szeroki zakres zmian względnej rezystancji obciążenia $r = R_o/R_n$ na zamieszczonych w artykule wykresach posłużono się skalą logarytmiczną. Badano wpływ zmian względnej rezystancji obciążenia r i kształtu sygnału zasilającego na względne straty mocy w uzwojeniach $p_u = \Delta P_u/\Delta P_{un}$ (rys. 2) i w rdzeniu $p_r = \Delta P_r/\Delta P_{rn}$ (rys. 3) oraz sprawność η transformatora (rys. 6). Przy obliczaniu sprawności uwzględniono straty histerezowe wyznaczone w sposób przybliżony na podstawie danych katalogowych. Sprawność tą porównano w pewnym zakresie obciążeń ze sprawności transformatora pracującego w zasilaczu impulsowym (rys. 4).

Opracowane oprogramowanie umożliwia analizę wiroprądowych strat mocy w uzwojeniach i rdzeniu transformatorów impulsowych. Zatem może być przydane w projektowaniu i optymalizacji rozpatrywanych transformatorów.